Applied Catalysis B: Environmental 243 (2019) 594–603

Contents lists available at ScienceDirect

Applied Catalysis B: Environmental

journal homepage: www.elsevier.com/locate/apcatb

Unexpected selectivity of ferrierite for the conversion of isobutanol to linear butenes and water effects

Z. Buniazet[a,b], A. Cabiac[b], S. Maury[b], D. Bianchi[a], S. Loridant[a,*]

[a] Institut de Recherches sur la Catalyse et l'Environnement de Lyon, IRCELYON, CNRS-Université Claude Bernard Lyon 1, 2 av. Einstein, F-69626, Villeurbanne Cedex, France

[b] IFP Energies nouvelles, Rond-point de l'échangeur de Solaize, BP 3, F-69360, Solaize, France

ARTICLE INFO

Keywords:
Bio-alcohols
Isobutanol
Bio-olefins
Butenes
Dehydration
Isomerization
Ferrierite zeolite
Acidic catalysts
Water effects

ABSTRACT

Ferrierite was shown to be highly efficient in the conversion of isobutanol to butenes with selectivity values higher than 98%. Furthermore, its isomerisation activity is remarkable since proportion of linear butenes higher than 80% was obtained in the present study confirming patents claims. This selectivity was shown to increase with temperature and contact time as well as with time on stream.

Neither water added to the feed nor water generated by dehydration has an impact on the structure of ferrierite as shown by XRD and ^{27}Al NMR. A slight enhancement of catalytic activity was observed below 250 °C and could be due to an increase in the number of BAS as suggested by *in situ* acidity measurements achieved at the reaction temperatures in presence of water vapor while competition of adsorption would inhibit the catalytic activity above 250 °C. Furthermore, water was shown to improve dramatically selectivity to linear butenes at low conversion. We propose that water inhibits the proton shift of isobutylcarbenium ions or deprotonation sites leading to isobutene but not acid sites able to isomerize isobutylcarbenium ions into linear carbocations leading to linear butenes. At high conversions, both coke formation and water generated by dehydration could improve selectivity to linear butenes by neutralization of unselective sites responsible for proton-shift reaction.

1. Introduction

The dehydration of biobased alcohols has gained much interest in the past two decades as a route to produce green olefins. Ethanol which can be dehydrated to ethylene and further transformed into polyethylene is the most promising bioalcohol but the dehydration of butanols has also received growing attention [1–3]. Indeed, developments in biotechnology have led to produce different butanol isomers by lignocellulosic biomass fermentation with acceptable yields. For instance, isobutanol can actually be seen as a potential feedstock as it is produced by Gevo since 2016 (1.5 Mgal/yr) at an acceptable price.

Kotsarenko et al. firstly studied the dehydration of isobutanol over silica based mixed oxides [4]. A significant proportion of linear butenes (33%) was obtained for most catalysts even those containing weak or moderated acid sites. A mechanism involving methyl-shift for the conjugated dehydration/isomerization of isobutanol to linear butenes was proposed. The selectivity to the different butenes was not affected by Brønsted acidity of WO_3/ZrO_2 catalysts [5] but the increased Brønsted acidity of aluminas containing low amounts of silica compared to pure aluminas was shown to significantly improve the selectivity to linear butenes [1]. The catalytic activity of $H_4SiW_{12}O_{40}$ heteropolyanions, WO_3 and TiO_2 supported on SiO_2 was related to the Brønsted acidity and selectivity to butenes close to 100% were obtained for the catalysts containing moderate and weak sites (WO_3/SiO_2 and TiO_2/SiO_2) [6]. It was proposed that the isomerisation activity is mainly related to the equilibrium between carbocations formed after E1 elimination of water for these catalysts leading to typically 35% of linear butenes at 300 °C. The slight increase in isomerisation activity observed for $H_4SiW_{12}O_{40}/SiO_2$ (and to a lesser extent for WO_3/SiO_2) was attributed to strong Brønsted acid sites able to catalyse the isomerization of isobutene to linear butenes.

Zeolites are efficient catalysts for the dehydration of butanols to butenes [2,3,7–10]. Note that isobutene was reported to be formed from linear butanols [2,3,9] or not [7,8,10]. Disassembling of ferrierite was shown to improve activity for the dehydration of 2-butanol [10]. Furthermore, zeolites casually modified by steaming or by phosphorus treatment were shown to achieve very efficiently the dehydration of isobutanol into the four butenes [11–13] using a feed isobutanol/H_2O = 95/5 at 200–400 °C temperature range and 1–3 bars. In particular, the proportion of linear butenes (n-butenes) was claimed to reach

* Corresponding author.
E-mail address: stephane.loridant@ircelyon.univ-lyon1.fr (S. Loridant).

https://doi.org/10.1016/j.apcatb.2018.11.007
Received 6 September 2018; Received in revised form 24 October 2018; Accepted 2 November 2018
Available online 03 November 2018
0926-3373/

56–59% using a ferrierite (H-FER) catalyst.

H-FER zeolite is a medium-pore zeolite composed of 10-membered rings (10-MR) with diameter 5.4 × 4.2 Å perpendicular and intersecting with 8-MR (3.4 × 4.7 Å). It is well known for its activity and high selectivity in skeletal isomerization of n-butene to isobutene [14–16]. As isobutene is slightly larger than the pore entrance of the 8-MR channels (kinetic diameter of 5.0 Å) [17], its diffusion is hindered with a high activation barrier contrarily to 10-MR (160 against 40 kJ.mol^{-1}) [18,19].

Young et al. compared the properties of ferrierite, ZSM-23 (10-MR of 5.2 × 4.5 Å), and ZSM-5 (10 MR of 5.6 × 5.3 Å and 5.5 × 5.1 Å) with Si/Al molar ratio of 8.8, 65 and 87, respectively in the n-butene isomerisation reaction [20]. The authors concluded that the key parameter is the size of both channels and interconnections and not acidity: the straight channels of ferrierite limit secondary reactions and their small sizes also prevent the formation of butene dimers. However, at short time on stream, it is commonly admitted by many authors that isomerization follows a bimolecular mechanism favoring dimerization and aromatization reactions [21,22].

Selectivity to isobutene is improved after partial deactivation of ferrierite by coke formation [23]. Such selectivation could be due either to poisoning of strong acidic sites or to increased steric stress limiting dimerization of n-butene. However, Seo et al. showed that the coke deposition, generated by plasma polymerization of propylene, did not have a significant influence on acidity and concluded that the improvement of isobutene selectivity is mainly due to steric hindrance limiting bimolecular reactions [14]. Only 10 MR channels would be effective for n-butene skeletal isomerisation while unselective 8 MR cages deactivate with time on stream [24]. By the use of STEM-EELS, De Jong et al. evidenced initial blocking of 8 MR channels even for low coke quantity. Their sensitivity to coking and ease to plug was explained by higher acid site density [25,26].

Interestingly, the isobutene yield decreased with time-on-stream while the linear butenes one increased when using ferrierite in the dehydration of n-butanol to butenes at 400 °C [3]. As this evolution was not observed in the isomerisation of n-butene [27,28], the authors proposed that water formed by dehydration (ca 25%) could modify the mechanism involved. However, addition of 5% H_2O at 320 °C during the conversion of linear butenes to isobutene had no impact on either conversion or selectivity which suggested that water effect depends both on temperature and water partial pressure [29].

Water can modify the catalytic activity of solid acid catalysts by irreversible textural and/or structural modifications, reactant solvation or competitive adsorption leading to a decrease in the number of catalytic sites, stabilization of intermediates and transition states, product dilution or solvation limiting consecutive reactions and coke formation and conversion of Lewis to Brønsted acid sites [30]. In the isomerization of n-butenes, water has been cofed to increase catalyst lifetime and isobutene selectivity [24].

In this study, ferrierite provided by Zeolyst (Product Name CP 914) was evaluated in the dehydration of isobutanol to butenes. The influence of reaction parameters such as temperature, contact time and time on stream as well as addition of water to the feed were investigated. Fresh and used samples were characterized by XRD, ^{27}Al NMR, ^{13}C CPMAS and TGA measurements. Textural properties were obtained from liquid N_2 adsorption/desorption isotherms and SEM images. Acidic properties were determined by NH_3-TPD, FTIR spectra after pyridine adsorption and from *in situ* acidity measurements achieved at the reaction temperatures in presence or not of water vapor.

2. Experimental part

2.1. Catalysts characterization

The molar Si/Al ratio was determined by WDXRF on a Perform'X from Thermofischer and Na amount from FAAS analysis on a Flame Spectraa 240 FS by Agilent Technologies. Textural properties were obtained by nitrogen physisorption at −196 °C using a Micromeritics ASAP 2020 instrument applying the BET and t-plot methods to determine specific surface area, micropores and external surface areas as well as micropore volumes. Scanning Electron Microscopy (SEM) micrographs were obtained with a FE-SEM JEOL 6340 F applying an acceleration voltage of 3 kV.

XRD patterns were achieved between 5 and 70° (2Θ) on a Bruker D8 Advance A25 diffractometer equipped with a Ni filter (Cu K_α radiation: 0.154184 nm) and a one-dimensional multistrip detector (Lynxeye, 192 channels on 2.95°). The International Center for Diffraction Data (ICDD) library was used for phase identification.

^{27}Al NMR measurements were carried out on a Bruker AVANCE III 500WB spectrometer operating at 130.29 MHz using a 4 mm triple probe. The spectra were recorded at 12 KHz spinning frequency with a pulse duration 0.5 µs (π/12), a recycle delay of 1 s over a spectral range of 400 ppm. The chemical shift was referenced to $Al(NO_3)_3$ 1 M. ^{13}C CPMAS measurements were carried on the same apparatus (125.73 MHz, pulse duration 3.5 µs (π/2), contact time 2 ms, recycle delay 5 s, 12 KHz spinning frequency) using a 4 mm triple probe. The chemical shift was referenced to adamantane.

NH_3-TPD curves were determined with Autochem II 2920 apparatus equipped with a TCD detector and a Pfeiffer mass spectrometer used to quantify only ammonia desorption and not water or impurities. 155 mg of ferrierite were pretreated at 500 °C for 2 h under helium, the temperature was then lowered to 150 °C. Ammonia adsorption was carried out for 30 min. Then after 30 min of purge under helium the temperature was increased up to 600 °C. The ammonia desorbed was quantified by means of TCD analyser. The integration of the signals gave the amount of acid sites as a function of temperature.

Acidity properties were also probed by adsorption of pyridine or NH_3 using homemade IR cells working in the pressure range 10^{-5}-1 bar. For all the measurements, self-supporting pellets (20 mg) were pretreated at 450 °C for 10 h under air flow which corresponded to the activation treatment before catalytic testings. Pyridine adsorption experiments were performed using a homemade IR cell equipped with CaF_2 windows. After cooling at RT, the sample was submitted to 4 mbar of pyridine. After desorption at increasing temperatures, transmission IR spectra were recorded at RT with Vector 22 (Bruker) spectrometer equipped with DTGS detector. The bands at 1446 and 1547 cm^{-1} were chosen for quantification of Lewis (LAS) and Brønsted (BAS) acid sites densities using extinction coefficient values of 1.50 and 1.67 cm.µ mol^{-1}, respectively [31–33]. *in situ* FTIR acidity measurements were performed with a Nicolet 6700 spectrometer (ThermoScientific) using a homemade stainless steel IR cell reactor specially designed to limit the gas phase contribution (its optical path is 2.2 mm) and NH_3 as probe molecule [34]. This IR cell allowed the study of adsorbed species in the range 20–450 °C under gas flow rates (200 mL.min^{-1} in the present study) of gas mixtures at atmospheric pressure such as x% NH_3/y% H_2O/He with x and y in the ranges 0–1% and 0–3% respectively. The amount of H_2O was controlled using a saturator/condenser system as described previously [35]. The density of BAS was quantified using an extinction coefficient of 8 cm.µ mol^{-1} for the $\delta_{asym}(NH_4^+)$ band [36].

2.2. Catalytic testing

After pretreatment of the ferrierite at 450 °C for 2 h under synthetic air flow (70 mL.min^{-1}), catalytic measurements were conducted at atmospheric pressure at temperatures ranging from 200 and 275 °C using an experimental set-up previously described in detail elsewhere [30] and summarized here: pure isobutanol (Aldrich, > 99.5%) was vaporized at 130 °C and diluted with a mixture of N_2 and CH_4 to obtain isobutanol partial pressure of 30%. CH_4 which was inert at the reaction temperatures and not a reaction product was used as internal standard. A solution of isobutanol containing 7 wt% H_2O (maximum amount without phase separation) was used to study the effect of water present

in the feed. The isobutanol partial pressure remained unchanged (30%) while the water vapor one was 10%.

The reaction mixture was sent to a fixed bed Pyrex reactor (16 mm diameter, 35 mm length) containing 250 mg of ferrierite. Catalytic performances were obtained combining off-line analysis (Shimadzu GC-2014, FID detector, Supelco column (30 m × 0.32 mm × 0.25 µm)) of trapped heavy products and unreacted isobutanol and online analysis (Shimadzu GC-2014, FID detector, Agilent HP-AL/KCL column (30 m × 0535 mm × 15 µm) of C1 to C5 hydrocarbons.

Reaction parameters such as temperature, 1/WHSV which is proportional to contact time, time on stream and water addition were investigated. Carbon balance values between 98 and 102% were obtained which ensured high quality of the catalytic measurements.

The following formulas were used to calculate the conversion, yields and selectivity set and carbon balance:

$$\text{Conversion}\ (\%) = \frac{\text{moles of reactant in} - \text{moles of reactant out}}{\text{moles of reactant in}}$$

$$Y_{product}\ (\%) = 100 \times K \times \frac{\text{moles of product}}{\text{moles of reactant in}} \text{with } K = \frac{\text{number of carbons in product}}{4}$$

$$S_{product}\ (\%) = 100 \times \frac{Y_{product}}{\text{Conversion}}$$

$$\text{Carbon balance}\ (\%) = \sum Y_{product}\ (\%) + 100 - \text{Conversion}\ (\%)$$

The isomerization activity was related to the proportion of linear butenes among butenes:

$$\%_{LinBut}\ (\%) = 100 \times \frac{S_{1-butene} + S_{cis-2-butene} + S_{trans-2-butene}}{\sum S_{butenes}}$$

Finally, reaction rates were calculated at different temperatures considering a plug-flow reactor and assuming a reaction order of 1 and were used to determine activation energies.

3. Results

3.1. Characterization of fresh ferrierite

The Si and Al contents of the zeolite measured by XRF were 42.7 and 2.1% respectively (Si/Al molar ratio 20). The measured Na amount was 127 ppm. The BET specific surface area was 389 $m^2.g^{-1}$ while the microporous one was 370 $m^2.g^{-1}$, the difference between the two values (19 $m^2.g^{-1}$) corresponding to intergranular porosity. SEM images (Figure S1, supporting information) revealed micro-sized aggregates consisting of rectangle plate-like primary particles of 500 nm to 4 µm long and 100 nm thick [37,38].

The XRD pattern of fresh ferrierite plotted in Fig. 1a fitted well with the ICDD 04-017-8702 reference (Immm structure, Z: 36, a: 18.90 Å, b: 14.13 Å and c: 7.44 Å) [39,40]. Its ^{27}Al NMR spectrum provided in Figure S2a contained one main band at 54.52 ppm typical of tetrahedral Al^{3+} cations and a very minor one at 0.04 ppm corresponding to octahedral Al^{3+} extraframework cations present in proportion lower than 1% [41–43].

The NH_3-TPD curve of fresh ferrierite (Figure S3) exhibited two peaks at 264 and 542 °C corresponding to weak and strong acid sites [38,43] with densities of 225 and 595 µmol. g^{-1}, respectively.

Fig. 2 shows the FTIR spectral evolution of fresh ferrierite from 450 down to 140 °C under 0.5%NH_3-He flow. The 2300-3800 cm^{-1} spectral range was not observable due to too weak IR transmission. Fig. 2 reveals the presence of both Lewis ($\delta_{asym}(NH_3)$ band at 1619 cm^{-1}) and Brønsted ($\delta_{asym}(NH_4^+)$ band at 1460 cm^{-1} at 140 °C) sites [44–46]. The bands between 1700 and 2200 cm^{-1} were attributed to combinaisons of $\delta(NH_4^+)$ bending modes with frustrated rotations [46]. The $\delta_{asym}(NH_4^+)$ band observed at 1426 cm^{-1} at 450 °C slightly shifted to

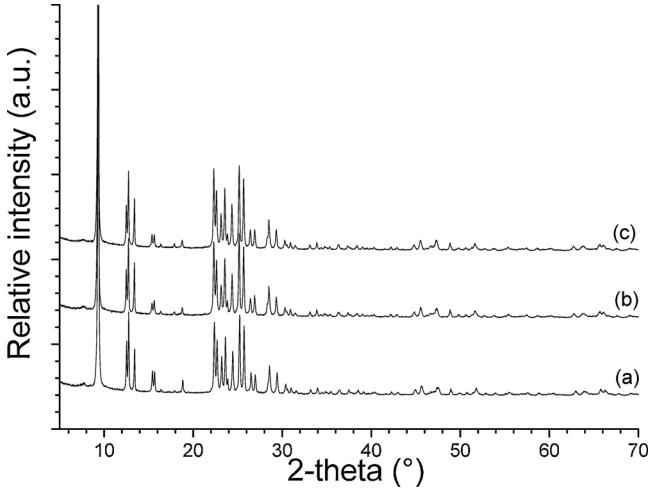

Fig. 1. XRD patterns of ferrierite (a) at the fresh state, (b) after 25 h under iC_4OH/inert: 30/70 feed at 250 °C, 1/WHSV 0.07 h and (c) after 25 h under iC_4OH/H_2O/inert: 30/10/60 feed at 250 °C, 1/WHSV 0.07 h.

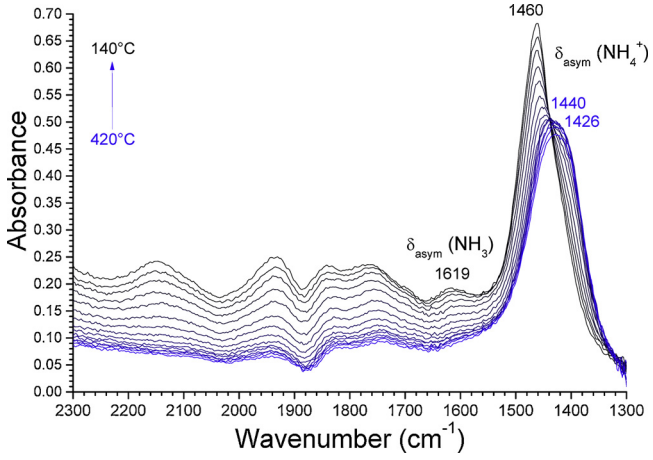

Fig. 2. FTIR spectra of ferrierite recorded from 450 down to 150 °C under 0.5% NH_3/He flow. The backgrounds correspond to the spectra recorded under He flow at the same temperatures, mass of the pellet 20 mg.

1440 cm^{-1} decreasing the temperature to 270 °C and shifted faster to 1460 cm^{-1} cooling down to 140 °C. In fact, this band contained three individual components (see Figure S4) revealing symmetry lowering from Td from Cs. It suggested the presence of tridentate or tetradentate species due to strong interaction between NH_4^+ and O^{2-} anions able to distord the ammonium ions [46]. Hence, the band at 1426 cm^{-1} corresponding to undistorded ammonium ions at 450 °C is replaced by an intense band at 1460 cm^{-1} corresponding to distorded ammonium ions at lower temperature. Considering that the extinction coefficient of the $\delta_{asym}(NH_4^+)$ band remained constant between 140 and 450 °C, the NH_4^+ surface density only decreased from 560 to 414 µmol. g^{-1} which was explained by the presence of strong BAS. The low temperature value was in good agreement with the number of Al^{3+} cations (674 µmol.g^{-1}) indicating that almost all of them generated H^+ protons probed by NH_3 molecules. Concerning the $\delta_{asym}(NH_3)$ band near 1619 cm^{-1} corresponding to LAS, its evolution with the temperature, which is related to the LAS strength was hard to follow because of its weakness and its superimposition with other bands.

LAS and BAS were well distinguished in the FTIR spectrum recorded after pyridine adsorption (Figure S5). The 8a band at 1619 cm^{-1} indicated the presence of strong LAS corresponding to tetrahedral Al^{3+} cations [44,47] while the high relative intensity of the 8a and 19b bands located at 1637 and 1545 cm^{-1}, respectively confirmed the high

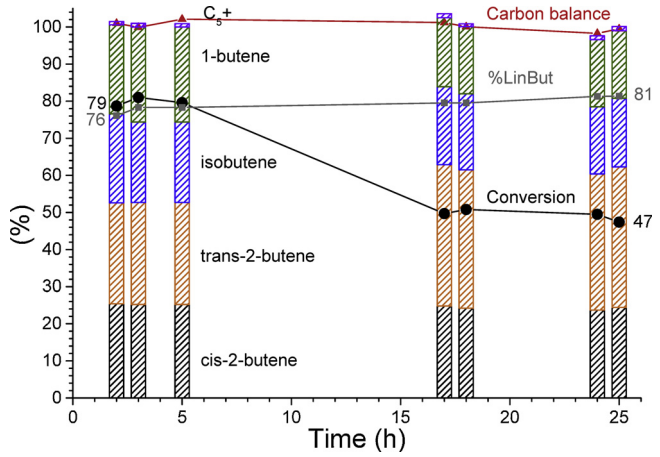

Fig. 3. Evolution with the time on stream of the conversion, the selectivity to butenes and %LinBut values and the carbon balance for ferrierite at 250 °C, iC_4OH/inert : 30/70 and 1/WHSV 0.07 h.

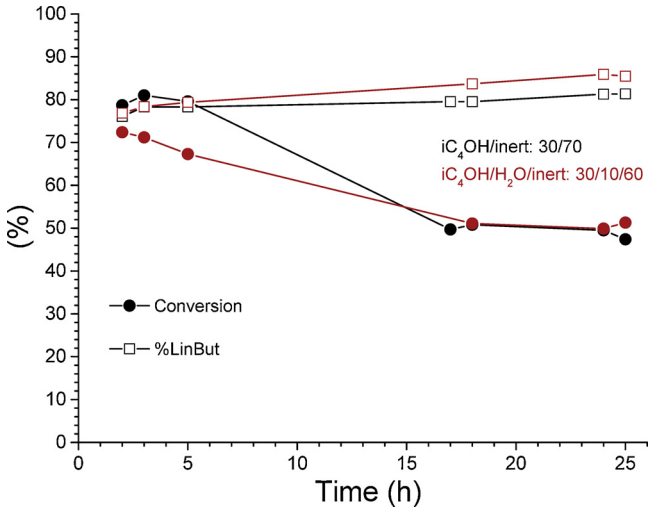

Fig. 4. Comparison of the evolutions with time on stream of the conversion and the %LinBut value for ferrierite sample under iC_4OH/inert: 30/70 (black curves) or iC_4OH/H_2O/inert: 30/10/60 (red curves) at 250 °C and 1/WHSV 0.07 h.

density of BAS. Indeed, density values of 20.9 and 104.7 μmol. g^{-1} were calculated for LAS and BAS respectively after desorption at 150 °C. The much lower values compared to NH_3 adsorption was explained by steric hindrance of pyridine (dynamic diameter of 5.22 Å versus 3.10 Å for NH_3). Hence, pyridine is not able to enter the ferrierite pores and probes only the external surface of ferrierite [48]. The ν(O−H) band at 3593 cm^{-1} was attributed to Si−OH−Al groups [42,48] and its negative absorbance was related to reaction of such acidic protons with pyridine leading to formation of pyridinium cations. The ν(O−H) band at 3747 cm^{-1} was attributed to Si−OH [42,48] and its negative absorbance could arise from H-bonding with pyridine leading to a shoulder at 1611 cm^{-1} [49].

3.2. Catalytic performances

Fig. 3 shows the evolutions of isobutanol conversion, selectivity and proportion of linear butenes (%LinBut value) as well as carbon balance with time on stream at 250 °C. Ferrierite was very selective to butenes with mean selectivity value higher than 98% over 24 h. The selectivity to C5+ compounds (mainly C8) was less than 1% and the one to cracking products was negligible in comparaison to selectivity reported for isomerization of butenes [14,16,23,27]. No trace of isobutane or any other alkane was detected which suggested the absence of hydrogen transfer reactions. Furthermore, the %LinBut value was 76% which is much higher than those measured for $H_4SiW_{12}O_{40}$, WO_3, TiO_2 and SnO_2/SiO_2 catalysts (value in the range 25–32%) [6,30] and close to values reported in patent literature at 300 °C (see [12,13] and related patents).

Ferrierite deactivated rapidly during the first hours of testing with a conversion drop from 79 to 50% during the first 18 h and then stabilized around 50-47% during the last 7 h. In parallel, the selectivity to trans-2-butene increased from 27 to 38% to the detriment of the ones to 1-butene and isobutene with a decrease from 24 to 18%. The selectivity in cis-2-butene remained almost unchanged. It led to a %LinBut value of 81% which is the best value reported up to now at 250 °C. Note that the carbon balance remained close to 100% during the catalytic testing period suggesting that a small amount of coke was sufficient to deactivate the catalyst.

3.3. Water effects on catalytic properties

Fig. 4 compares the evolutions at 250 °C over time on stream of the isobutanol conversion and %LinBut values for feed containing 10 or 0% of water at 1/WHSV 0.07 h: the conversion was higher using water free feed during the first 6 h but it became equivalent upon deactivation after 15 h. It implies that the deactivation rate was lower in the presence of water. Interestingly, the %LinBut value increased and even reached a higher value with 10%H_2O feed than with water free feed (85 vs 81% after 24 h). Hence, selectivation is significantly favoured by the presence of water suggesting it neutralizes unselective sites.

Fig. 5 compares the evolutions of the isobutanol conversion and % LinBut values with reaction temperature for feed containing 10% or 0% of water at 1/WHSV 0.07 h. Each data corresponds to a test carried out with a fresh catalyst and is an average of two values obtained during 4 h of testing in order to limit the effects of selectivation. Note that the values obtained at 250 °C were close to the ones plotted in Figs. 3 and 4 at short time on stream and corresponding to another reactor loading. This pointed out the repeatability of catalytic measurements. It was found from Fig. 5 that the effect of water on the conversion depends on the reaction temperature with a positive effect below 250 °C and a negative one above, i.e. for high conversions. Anyway, the activation energies Ea calculated from the Arrhenius plots and provided in Figure S6 were rather close to each other with values of 101 and 112 kJ.mol^{-1} for feed without and with water addition, respectively. It suggested that the active sites were of the same nature in both cases. By comparison, they were much more efficient than active sites present in TiO_2/SiO_2

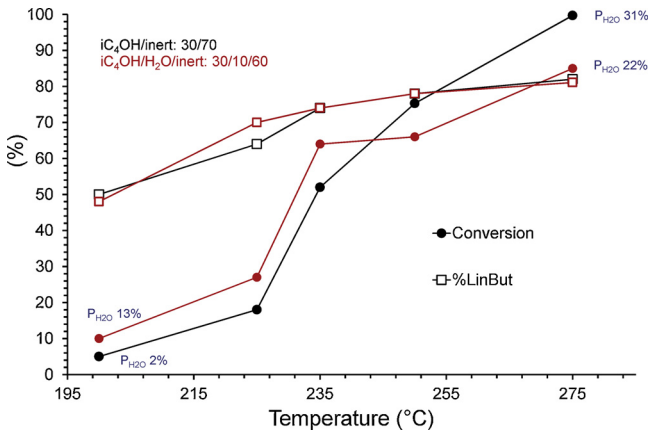

Fig. 5. Comparison of the evolutions with reaction temperature of the conversion and the %LinBut value for ferrierite under iC_4OH/inert: 30/70 (black curves) or iC_4OH/H_2O/inert: 30/10/60 (red curves) at 1/WHSV 0.07 h. The partial pressures of water in the reactor are reported in blue.

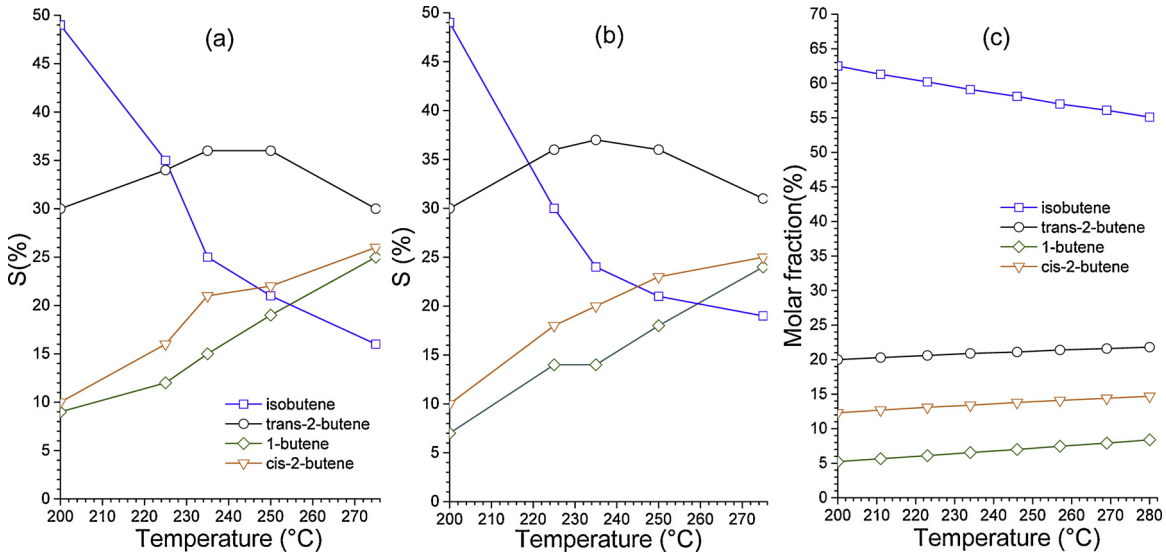

Fig. 6. Evolutions with temperature of the selectivity to butenes obtained for ferrierite under (a) iC_4OH/inert:30/70 and (b) iC_4OH/H_2O/inert:30/10/60 at 1/WHSV 0.07 h and (c) evolution of the butenes molar fraction with temperature calculated with the HSC Chemistry Software.

catalysts (Ea 145 kJ.mol^{-1}) [30] but similar to those present in 10%Al_2O_3-90%SiO_2 (Ea 100 kJ.mol^{-1}) [4] for instance.

The %LinBut value strongly increased with the reaction temperature from 50% at 200 °C to 82% at 275 °C. However, no effect of water addition was observed on the selectivity contrarily to the conversion. As shown in Fig. 6, the evolution of selectivity was quite similar for the two feeds with a strong decrease in the selectivity to isobutene to the benefit of cis-2-butene and 1-butene while the selectivity to trans-2-butene increased up to 240 °C and decreased above 250 °C (small optimum around 240 °C). This evolution with temperature reminds the one corresponding to thermodynamic equilibrium of butenes (see the molar ratios in Fig. 6c) except for trans-2-butene. Furthermore, the absolute values and slopes are different. At 246 °C, expected equilibrium values between butenes are as follows: 57% for isobutene, 21% for trans-2-butene 14% for cis-2-butene and 7% for 1-butene while they are 55%, 22%, 15% and 8%, respectively at 280 °C. The similarity of evolution suggested that water influences the number of sites but not their nature as already pointed out from activation energy calculations.

The evolution curves of the isobutanol conversion and %LinBut values at 250 °C are plotted versus the 1/WHSV parameter in Fig. 7 for 10% H_2O or water free feed. Given the rather fast deactivation of ferrierite, the catalytic properties were evaluated two times using two loadings: a first one for long contact times (1/WHSV = 0.06-0.09 h, measurements duration: 9 h) and a second one for shorter contact times (1/WHSV = 0.03-0.04 h, measurements duration: 6 h). As said previously for 1/WHSV 0.07 h (Fig. 4) the addition of water has a negative effect on the conversion of fresh ferrierite at 250 °C regardless the 1/WHSV value suggesting some adsorption competition with isobutanol. Note that the error bars determined from repeatability measurements were lower than the differences of conversion measured for the feed with and without water. However, the isomerisation activity was much higher when adding water to the feed at low contact time corresponding to low conversion: for instance, the % LinBut value was 79% with the feed containing water and only 68% with the water free feed at 1/WHSV 0.03 h. Furthermore, this value was rather constant with increase in 1/WHSV value while it significantly increased for water free feed. As such difference could be explained by different butenes adsorption-desorption equilibria, conversion-selectivity curves were plotted for the two feeds (Fig. 8). In the absence of water, the selectivity to trans-2-butene was constant around 36% while the selectivity to isobutene decreased of ca 10% to the benefit of cis-2-butene and 1-butene (Fig. 8a) in agreement with the evolution of the %LinBut value

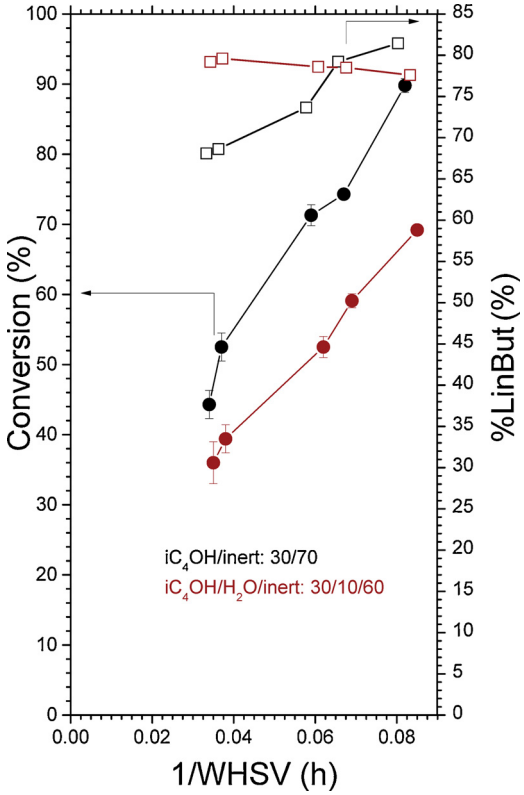

Fig. 7. Comparison of the evolutions with the 1/WHSV value of the conversion and the %LinBut value for ferrierite under iC_4OH/inert: 30/70 (black curves) or iC_4OH/H_2O/inert: 30/10/60 (red curves) at 250 °C.

(Fig. 7). Note that the selectivity values at 74% of conversion (1/WHSV 0.07 h) corresponded to slightly deactivated but selectivated catalyst considering the data plotted in Fig. 3. When water was added to the feed (Fig. 8b), the selectivity values remained almost constant with conversion and were close to the ones obtained at high conversion with water free feed. Hence, the proportion of linear butenes was almost constant (78–79%) increasing the conversion when water was added to the feed while it increased for free water feed reaching similar values (Figure S7). It suggested that water formed by the dehydration reaction

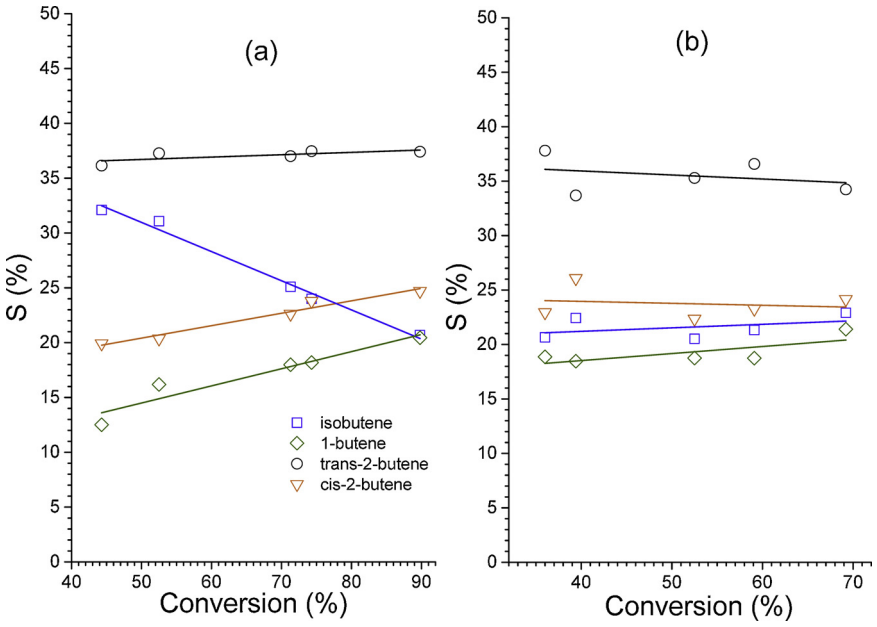

Fig. 8. Conversion-Selectivity curves obtained for ferrierite under (a) iC_4OH/inert: 30/70 and (b) iC_4OH/H_2O/inert: 30/10/60 at 250 °C, 1/WHSV: 0.03-0.08 h.

at high conversion led to similar selectivation than water added to the feed. Note also that higher amount of coke is formed at higher conversion which could also contribute to selectivation.

3.4. Water effect on acidic properties

The water effect on the ferrierite acidic properties was investigated from *in situ* acidity measurements achieved at the adsorption equilibrium using 1%NH_3/3%H_2O/He flows in a temperature range of interest for the catalytic reaction. The spectra were compared to those recorded under 1%NH_3/He in Fig. 9. Below 270 °C, the presence of water molecules adsorbed on the surface of ferrierite was clearly observed with the contribution of an IR band $\delta(H_2O)$ at 1619 cm^{-1} superimposed on the $\nu_{asym}(NH_3)$ band of NH_3 species adsorbed on LAS. In parallel, the intensity of the $\delta_{asym}(NH_4^+)$ band at 1460 cm^{-1} increased in the presence of water. Below 100 °C, such phenomenon can not be attributed unambiguously to an increase in BAS because the reaction:

$$NH_3 + H_2O_{ads} => NH_{4ads}^+ + OH_{ads}^-$$

can occur between the physisorbed water and NH_3 [30,35]. Above 100 °C, the intensity of the band at 1426 cm^{-1} was almost unchanged by the presence of water while the IR band of the chimisorbed water decreased regularly. The similarity of the NH_4^+ band for both experiments showed that the addition of water to the feed has no significant effect on the BAS density for catalytic testing carried out above 250 °C. It also implies that their strength remained unchanged. Note that formation of BAS were clearly evidenced for TiO_2/SiO_2 catalyst from such *in situ* FTIR acidity measurements which explained the catalytic activity improvement adding water to the feed between 200 and 300 °C [30].

3.5. Structural and textural characterization of ferrierite after reaction

The diffractograms of ferrierite samples tested for 25 h at 250 °C, 1/WHSV 0.07 h under feeds containing water or not (Fig. 1c and b, respectively) were identical to the fresh sample one (Fig. 1a) showing that the Immm crystalline structure [41] was maintained. The Al^{3+} coordination was also unchanged since the ^{27}Al NMR spectrum recorded after testing mainly consisted of one band around 54 ppm corresponding to tetrahedral Al^{3+} [41–43]. The small shift (from 54.52–53.45 ppm) and the small amplitude decrease could be due to slight change of distorsion [50] linked to different adsorbed molecules

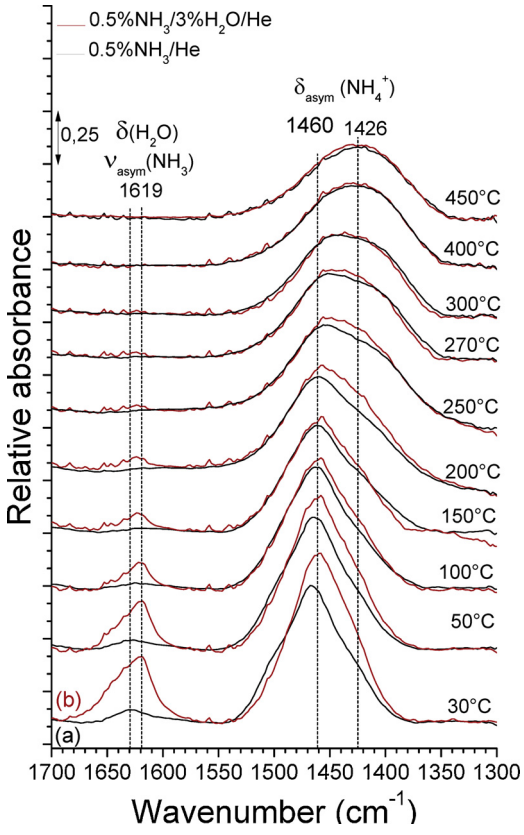

Fig. 9. Comparison of the evolution of FTIR spectra of ferrierite recorded from 450 to 30 °C under (a) 1% NH_3/He and (b) 1% NH_3/3%H_2O/He. The backgrounds correspond to the spectra recorded under He flow at the same temperatures, mass of the pellet 20 mg.

between the fresh and aged states. Note also that the very weak band at 0.04 ppm band corresponding to octahedral Al^{3+} cations [41–43] was not observed after reaction. Thus, the coordination of Al^{3+} cations was not modified either by the pretreatment at 450 °C or by exposure to water vapor formed by dehydration at 250 °C for 25 h. In particular, no Al^{3+} extraframework cation was formed by steaming during the

Table 1
Textural properties obtained from N_2 liquid temperature adsorption and t-plot measurements for fresh and used ferrierite samples. The used catalysts were tested for 6 h under feed at 1/WHSV 0.07 h.

		t-plot surface area ($m^2.g^{-1}$)	t-plot porous volume ($cm^3.g^{-1}$)
Fresh catalyst		370	0.15
Used catalyst			
Temperature (°C)	Feed composition		
235	iC_4OH/H_2O/inert = 30/10/60	285	0.12
	iC_4OH/inert = 30/70	295	0.12
275	iC_4OH/H_2O/inert = 30/10/60	280	0.11
	iC_4OH/inert = 30/70	290	0.12

reaction. Note that steam treatments reported in ref.11 and leading to formation of extra framework aluminium were achieved above 400 °C.

The N_2 physisorption isotherms of ferrierite sample tested for 6 h at 235 and 275 °C using feeds containing water or not were achieved. It was necessary to pretreat the solids for 3 h at 350 °C under vacuum before the measurements which could remove adsorbed molecules corresponding to soft coke. The surface areas and the porous volumes reported in Table 1 were significantly lower than the values obtained for fresh ferrierite. This textural change was due to coke deposit inside the micropores of the ferrierite zeolite [43,51] which was not removed by the desorption pretreatment. However, the values were quite similar for the four samples showing that water has no effect on the modifications of textural properties by coking when reaction is conducted at both 235 and 275 °C.

3.6. Water effect on coke formation

In order to determine the water effect on coke formation, ferrierite samples tested for 6 h at 235 and 275 °C using feeds containing water or not were analysed by ^{13}C NMR and TGA. The NMR spectra plotted in Fig. 10 contained bands between 10 and 100 ppm corresponding to aliphatic carbons while those around 125 and 160 ppm corresponded to CO and CH bonds in aromatic structures, respectively [52–54]. It appeared that ferrierite mainly forms aliphatic coke when tested at 235 °C with and without the addition of water. On the other hand, the presence of both aliphatic and aromatic coke was clearly observed after testing at 275 °C. Even though NMR spectroscopy is not quantitative, it is worth noting that the relative intensity of the bands corresponding to the aliphatic coke seems much lower in the presence of water which suggested that its formation is then limited.

TGA measurements were performed up to 700 °C on the four spent solids. The spent zeolites were brown before the measurements and

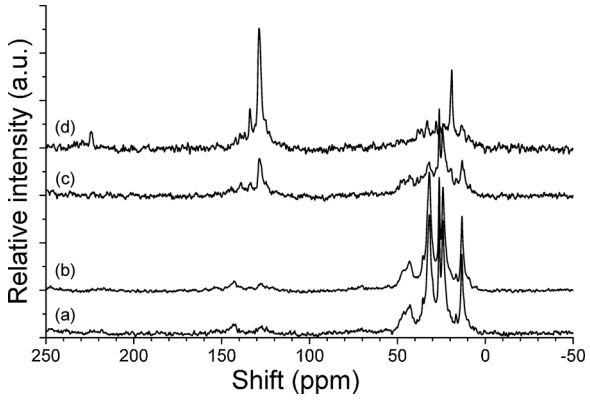

Fig. 10. ^{13}C solid NMR spectra of ferrierite after 6 h of reaction (a) at 235 °C under iC_4OH/inert: 30/70 (b) 235 °C, iC_4OH/H_2O/inert: 30/10/60, (c) 275 °C, iC_4OH/inert: 30/70 and (d) 275 °C, iC_4OH/H_2O/inert: 30/10/60. The 1/WHSV value was 0.07 h in all cases.

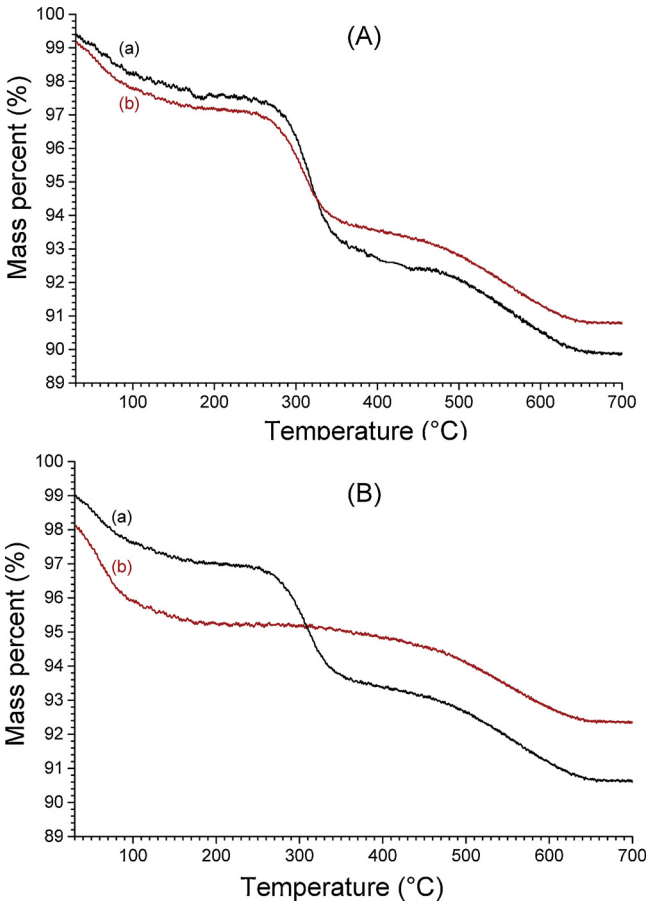

Fig. 11. TGA curves of ferrierite after 6 h of reaction (A) at 235 °C, 1/WHSV: 0.07 h under (a) iC_4OH/inert: 30/70 or (b) iC_4OH/H_2O/inert: 30/10/60, (B) at 275 °C, 1/WHSV: 0.07 h under (a) iC_4OH/inert: 30/70 or (b) iC_4OH/H_2O/inert: 30/10/60.

became white (color of the fresh ferrierite) after. This indicated that most carboneous compounds have been burned at 700 °C. The curves plotted in Fig. 11 started with a small loss of water between 25 and 150 °C accounting for about 3 wt%. The second mass loss of 4 wt% observed between 150 and 350 °C was attributed to aliphatic coke and/or to adsorbed organic molecules in agreement with NMR spectra. Interestingly, it was not observed for the catalyst tested at 275 °C with water added to the feed. A third mass loss of about 3 wt.% corresponding to oxidation of aromatic coke [55–58] was observed between 350 and 650 °C. It revealed that aromatic coke was present in equivalent amount for the four spent samples even though hardly detected by NMR when testing at 235 °C. Interestingly, the amounts of coke were close (ca 7%) for the two reaction temperatures and free water feed in spite of different conversions (52 and 100% at 235 and 275 °C,

respectively) showing that the overall coking rate was the same. Note that considering the testing time (6 h), the quantities of coke corresponded to low coking rates in line with the high carbon balances (> 98%) determined from GC measurements.

In summary, it appeared that the TGA curves were quite similar for catalysts tested at 235 °C with the two different feeds and suggested that the added water had no influence on the coke formation under these conditions. On the contrary, addition of water limited formation of aliphatic coke and/or adsorption of organic molecules for catalysts tested at 275 °C.

4. Discussion

Ferrierite appeared to be more active than 20.4%TiO_2/SiO_2 catalyst [30] but less than 18.5%$H_4SiW_{12}O_{40}/SiO_2$ and 39.7%WO_3/SiO_2 [6] in the dehydration of pure isobutanol. BAS are active in the isobutanol dehydration via E1 elimination mechanism [4,6]. The large difference of BAS density probed either by NH_3 or pyridine (560 vs 105 μmol. g^{-1}) for ferrierite arises from large difference of kinetic diameter between the two probes (2.6 vs 5.9 Å, [59,60]). Note that the kinetic diameter of isobutanol (5.5 Å, [61]) is close to the one of pyridine which strongly suggests that only a very limited part of ferrierite is active in the dehydration step. However, the density of BAS determined from pyridine adsorption was higher for ferrierite sample (105 μmol. g^{-1}) than for 18.5%$H_4SiW_{12}O_{40}/SiO_2$ (55 μmol. g^{-1}) and 39.7%WO_3/SiO_2 (10 μmol. g^{-1}) supported catalysts in spite of a lower activity. It suggested that stronger and more active BAS were present in the two non zeolitic catalysts.

Ferrierite led to high selectivity to butenes (> 98.5%) with a limited selectivity to C5+ compounds even at short time on stream. On the contrary, a selectivity to C5+ products of 10% was estimated for 18.5% $H_4SiW_{12}O_{40}/SiO_2$ with uncomplete carbon balance at short time of stream [6]. This difference of selectivity could be explained by a limited number of accessible strong BAS in ferrierite, thus preventing the dimerisation of butenes and by stronger acid sites on 18.5%$H_4SiW_{12}O_{40}/SiO_2$. Note that a remarkable selectivity for ferrierite was also pointed out in the skeletal isomerization of isobutene to n-butenes with selectivity value of 95% at similar contact time (1/WHSV 0.07 h) and isobutene partial pressure (30 vol%) [16]. The absence of oligomerization over ferrierite led to the absence of oligomers cracking therefore suppressing the formation of C3 and C5 molecules and favoured high selectivity.

Furthermore, the high %LinBut values (> 80%) obtained with ferrierite of Si/Al 20 studied in this work confirmed patents claims [12,13]. Such unexpected selectivity to linear butenes underlined the interest to use ferrierite in the dehydration of isobutanol. Interestingly, the %LinBut parameter was shown to strongly increase with temperature (Fig. 5) and moderately with 1/WHSV (Fig. 7). It also slightly increases with time on stream in spite of decrease in conversion.

Selectivity to butenes was a complex function of temperature, contact time and time on stream: for instance, selectivity to trans-2-butene strongly increases with time on stream but not with temperature nor conversion while selectivity to 1-butene strongly increases with temperature and conversion but decreases moderately with time on stream. As 1-butene, cis-2-butene selectivity increases with temperature and conversion but was quite constant with time on stream. Selectivity to isobutene decreases with temperature, time on stream and contact time favoring linear butenes selectivity. For oxides supported on mesoporous silica, the linear butenes appeared as mainly formed from thermodynamic equilibrium between the four carbocations and trans-2-butene/1-butene and cis-2-butene/1-butene ratios close to 1 were obtained whatever the reaction parameters [4,6,30]. In the present work, they were shown to vary from 1.1 to 3.3 and 1.0 to 1.8, respectively evidencing that a particular isomerization mechanism was involved using isobutanol as reactant and ferrierite as catalyst. Ether mediated mechanisms to form linear butenes seem to be ruled out since the selectivity to ethers strongly decreases with temperature [62] and no ethers were detected in the present study.

For the isomerisation of n-butenes, it is commonly admitted in the litterature that the reaction follows a bimolecular mechanism favoring dimerization and aromatization reactions on fresh ferrierite prior to selectivation. The formation of coke leads thus to a mono or pseudo-mono-molecular mechanism which is more selective to isobutene [21–23].

In the dehydration of isobutanol, sites leading to isobutene formation appear to be less active (or numerous) after both long time on stream and at high conversion. This phenomenon could arise from coking which was shown to be significant after 6 h of testing at 235 and 275 °C (7%, Fig. 11A) or from water effects as discussed in the following paragraphs.

Various effects of water on the dehydration activity of zeolites are reported in the litterature: no effect was observed on either activity or selectivity in the dehydration of butanol isomers over H-ZSM5 up to a water content of ca. 20 mol% [9]. However, water was found to have a negative effect on the rates of both inter and intramolecular dehydration of 2-propanol and 2-butanol over X zeolite [7]. In the present study, a complex evolution of the catalytic activity of ferrierite with temperature was observed in the presence of water (Fig. 5). Textural or structural evolution of the ferrierite under water rich environnement was ruled out. The slight enhancement of activity below 250 °C could be due to a small increase in the number of BAS while the inhibition above 250 °C cannot be explained by a change of acidity. This phenomenon systematically observed at 250 °C whatever the contact time can be explained by competitive adsorption between water and isobutanol. Finally, water has a limited influence on the deactivation rate with time on stream (Fig. 4) and on the evolution of isomerisation activity with temperature (small increase, see Fig. 5).

For water free feed, the selectivity to isobutene decreased significantly to the benefit of 1-butene and cis-2-butene when going from 40% (low contact time) to 90% (high contact time) conversion (Fig. 8a) suggesting isobutene was a primary product. Remarkably, the proportion of linear butenes was much higher at low contact time (80 vs 68%) when adding water to the feed (Fig. 7) as a consequence of lower selectivity to isobutene and higher selectivity to 1-butene (Fig. 8b). In fact, the role of water could be to inhibit proton shift of isobutylcarbenium ions [4] or to saturate deprotonation sites responsible for the formation of isobutene. A same effect was observed for water formed *in situ* by the dehydration step but to a lesser extent (high conversion case). Note that water was shown to favor isobutene selectivity in the isomerization of n-butenes [24] which is the opposite of the present study. It also indicates that isobutene is not formed by consecutive isomerisation of n-butenes in our case.

In the presence of water, the butenes selectivity was almost constant with conversion (Fig. 8b) indicating different reaction mechanisms involving different sites could be at stake. In the presence of water, unselective sites would be inhibited, preventing the formation of isobutene. Furthermore, the addition of water was shown to limit the formation of soft coke (Figs. 10 and 11) which could also explain inhibition of isobutene formation leading to higher selectivity to linear butenes at least at high contact time and time on stream. At low contact time on fresh ferrierite, contribution of coke formation on selectivity to linear butenes would be negligible.

Hence, we can propose that accessible BAS of ferrierite dehydrate isobutanol to form isobutylcarbenium ions. The proton shift leading to isobutene favoured at a low contact time in the absence of water would be inhibited by water and formation of soft coke. Isobutylcarbenium ions could also diffuse and react on accessible and strong enough BAS to isomerize into linear carbocations by methyl shift. Such particular BAS (possibly located at pores mouth) are not affected by water and soft coke formation leading to high selectivity to linear butenes at high contact time and time on stream (Fig. 12).

Improvement of selectivity to linear butenes would then be due to

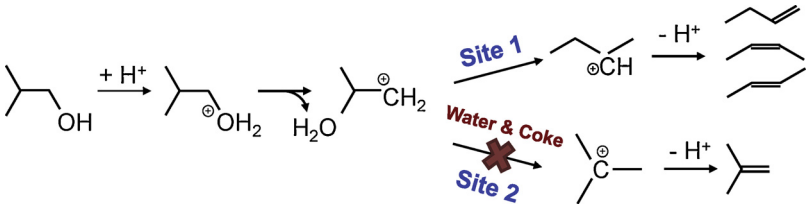

Fig. 12. Proposed reaction scheme in the dehydration of isobutanol to butenes over ferrierite zeolite.

water added in the feed, to water generated at high conversions (high contact times and high temperatures), and/or to coke formation (high contact times, high times on stream and high temperatures). Water or coke would both play a role by neutralizing unselective sites responsible for proton-shift reaction.

5. Conclusions

Ferrierite was shown to be highly efficient in the conversion of isobutanol to butenes. In particular, this study confirmed the high isomerisation activity claimed in patents for this reaction since proportion of linear butenes higher than 80% can be produced over ferrierite. It was shown to increase with temperature from 200 to 275 °C and contact time as well as with time on stream. In spite of limited quantity of C_5^+ products formed, ferrierite deactivates with time on stream which is associated with formation of aliphatic and aromatic coke.

The reason for this high selectivity is not quite understood yet and theoretical calculations (DFT, molecular dynamics, mechanistic study via microkinetic experiments) would be beneficial to go further. However, it appears that a limited number of BAS are accessible to dehydrate isobutanol into isobutylcarbenium cations. They can be rearranged to form directly isobutene or be isomerized into linear carbocations on strong and close enough BAS.

Water added or generated by dehydration had no impact on the textural and structural properties of ferrierite under the reaction conditions and for the duration studied. However, it influenced the catalytic activity positively below 250 °C and negatively above probably by competitive adsorption between water and isobutanol. Heat adsorption measurements have been undertaken to confirm this assumption and will be published in forthcoming paper. Furthermore, water was shown to inhibit isobutene formation leading to remarkly high selectivity to linear butenes at low contact time. At high conversions, both coke formation and water generated could lead to such selectivation by neutralization of unselective sites responsible for proton-shift reaction.

Acknowledgments

This work has been cofounded by INC/CNRS (Z. Buniazet PhD thesis grant) and IFP Energies Nouvelles.

Appendix A. Supplementary data

Supplementary material related to this article can be found, in the online version, at doi:https://doi.org/10.1016/j.apcatb.2018.11.007.

References

[1] J.D. Taylor, M.M. Jenni, M.W. Peters, Top. Catal. 53 (2010) 1224–1230.
[2] D. Zhang, S.A.I. Barri, D. Chadwick, Appl. Catal. A Gen. 403 (2011) 1–11.
[3] D. Zhang, R. Al-Hajri, S.A.I. Barri, D. Chadwick, Chem. Commun. (Camb.) 46 (2010) 4088–4090.
[4] N.S. Kotsarenko, L.V. Malysheva, Kinetika i Kataliz 24 (1983) 877–882.
[5] E. Hong, H.-I. Sim, C.-H. Shin, Chem. Eng. J. 292 (2016) 156–162.
[6] Z. Buniazet, C. Lorentz, A. Cabiac, S. Maury, S. Loridant, Mol.Catal. 451 (2018) 143–152.
[7] P.A. Jacobs, M. Tielen, J.B. Uytterhoeven, J. Catal. 50 (1977) 98–108.
[8] P. Tynjälä, T. Pakkanen, S. Mustamäki, J. Phys. Chem. B 102 (1998) 5280–5286.
[9] D. Gunst, K. Alexopoulos, K. Van Der Borght, M. John, V. Galvita, M.-F. Reyniers, A. Verberckmoes, Appl. Catal. A Gen. 539 (2017) 1–12.
[10] S. Jeong, H. Kim, J.-H. Bae, D. H. Kim, C.H.F. Peden, Y.-K. Park, J.-K. Jeon, Catal. Today 185 (2012) 191–197.
[11] C. Adam, D. Minoux, N. Nesterenko, S. Van Donk, J.-P. Dath, Patent US20130204057 A1.
[12] T. Vivien, S. Maury, V. Coupard, D. Bazer-Bachi, N. Nesterenko, N. Danilina, Patent WO 2016/046242 A1.
[13] N. Nesterenko, C. Dupont, V. Coupard, S. Maury, T. Heinz, Patent WO2018/046516 A1.
[14] G. Seo, H.S. Jeong, D.-L. Jang, D.L. Cho, S.B. Hong, Catal. Lett. 41 (1996) 189–194.
[15] G. Seo, H.S. Jeong, S.B. Hong, Y.S. Uh, Catal. Lett. 36 (1996) 249–256.
[16] G. Seo, S.-H. Park, J.-H. Kim, Catal. Today 44 (1998) 215–222.
[17] B. Wichterlova, N. Zilkova, E. Uvarova, J. Cejka, P. Sarv, M.C. Paganini, J.A. Lercher, Appl. Catal. A: Gen. 182 (1999) 297–308.
[18] R. Millini, S. Rossini, Stud. Surf. Sci. Cat. 105 (1997) 1389–1396.
[19] F. Jousse, L. Leherte, D.P. Vercauteren, Mol. Sim. 17 (1996) 175–196.
[20] C.L. O'Young, R.J. Pellet, D.G. Casey, J.R. Ugolini, R.A. Sawicki, J. Catal. 151 (1995) 467–469.
[21] K.P. de Jong, H.H. Mooiweer, J.G. Buglass, P.K. Maarsen, Stud. Surf. Sci. Catal. 111 (1997) 127–134.
[22] S. van Donk, E. Bus, A. Broersma, J.H. Bitter, K.P. de Jong, Appl. Catal A: Gen. 237 (2002) 149–159.
[23] W.-Q. Xu, Y.-G. Yin, S.L. Suib, J.C. Edward, C.-L. O'Young, J. Phys. Chem. 99 (1995) 9443–9452.
[24] L. Domokos, L. Lefferts, K. Seshan, J.A. Lercher, J. Mol. Catal. A Chem. 162 (2000) 147–157.
[25] S. van Donk, F.M.F. Sander, O. de Groot, J.H. Stephan, K.P. Bitter, Jong de, Chem. A Eur. J. 9 (2003) 3106–3111.
[26] V.L. Zholobenko, D.B. Lukyanov, J. Dwyer, W.J. Smith, J. Phys. Chem. B 102 (1998) 2715–2721.
[27] R. Byggningsbacka, N. Kumar, L.E. Lindfors, J. Catal. 178 (1998) 611–620.
[28] W.Q. Xu, Y.G. Yin, S.L. Suib, J.C. Edwardsand, C.L. Oyoung, J. Catal. 163 (1996) 232–244.
[29] J. Zhang, R. Ohnishi, Y. Kamiya, T. Okuhara, J. Catal. 254 (2008) 263–271.
[30] Z. Buniazet, J. Couble, D. Bianchi, M. Rivallan, A. Cabiac, S. Maury, S. Loridant, J. Catal. 348 (2017) 125–134.
[31] I.S. Pieta, M. Ishaq, R.P.K. Wells, J.A. Anderson, Appl. Catal. A Gen. 390 (2010) 127–134.
[32] M. Tamura, K. Shimizu, A. Satsuma, Appl. Catal. A Gen. 433–434 (2012) 135–145.
[33] C.A. Emeis, J. Catal. 141 (1993) 347–354.
[34] T. Chafik, O. Dulaurent, J.L. Gass, D. Bianchi, J. Catal. 179 (1998) 503–514.
[35] F. Giraud, J. Couble, C. Geantet, N. Guilhaume, E. Puzenat, S. Gros, L. Porcheron, M. Kanniche, D. Bianchi, J. Phys. Chem. C 119 (2015) 16089–16105.
[36] A. Vimont, J.-C. Lavalley, L. Francke, A. Demourgues, A. Tressaud, M. Daturi, J. Phys. Chem. B 108 (2004) 3246–3255.
[37] Y. Hu, C. Xu, H. Zhang, Y. Wang, J. Deng, H. Zhang, Chem. Select 2 (2017) 3408–3413.
[38] S.C.C. Wiedemann, A. Muñoz-Murillo, R. Oord, T. van Bergen-Brenkman, B. Wels, P.C.A. Bruijnincx, B.M. Weckhuysen, J. Catal. 329 (2015) 195–205.
[39] I. Bull, P. Lightfoot, L.A. Villaescusa, L.M. Bull, R.K.B. Gover, J.S.O. Evans, R.E. Morris, J. Am. Chem. Soc. 125 (2003) 4342–4349.
[40] S.J. Weigel, J.-C. Gabriel, E. Guttierez Puebla, A. Monge Bravo, N.J. Henson, L.M. Bull, A.K. Cheetham, J. Am. Chem. Soc. 118 (1996) 2427–2435.
[41] J. Fraissard, R. Vincent, C. Doremieux, J. Kärger, H. Pfeiffer, J.R. Anderson, M. Boudart (Eds.), Catalysis: Science and Technology, 10 Springer, New York, 1996, pp. 52–57.
[42] K. Brylewska, K.A. Tarach, W. Mozgawa, Z. Olejniczak, U. Filek, K. Gora-Marek, J. Mol. Structure 1126 (2016) 147–153.
[43] H. Hu, M. Ke, K. Zhang, Q. Liu, P. Yu, Y. Liu, C. Li, W. Liu, RSC Adv. 7 (2017) 31535–31543.
[44] G. Busca, Phys. Chem. Chem. Phys. 1 (1999) 723–736.
[45] F. Giraud, C. Geantet, N. Guilhaume, S. Loridant, S. Gros, L. Porcheron, M. Kanniche, D. Bianchi, J. Phys. Chem. C 118 (2014) 15677–15692.
[46] A. Zecchina, L. Marchese, S. Bordiga, C. Pazè, E. Gianotti, J. Phys. Chem. B 101 (1997) 10128–10135.
[47] G. Busca, Catal. Today 41 (1998) 191–206.
[48] J.A.Z. Pieterse, S. Veefkind-Reyes, K. Seshan, L. Domokos, J.A. Lercher, J. Catal. 187 (1999) 518–520.
[49] C. Morterra, A. Chiorino, G. Ghiotti, E. Garrone, J. Chem. Soc. Faraday Trans. 1 (75) (1979) 271–288.
[50] A.P.M. Kentgens, K.F. Scholle, W.S. Veeman, J. Phys. Chem. 87 (1983) 4357–4362.
[51] S.C.C. Wiedemann, J.A. Stewart, F. Soulimani, T. van Bergen-Brenkman, S. Langelaar, B. Wels, P. de Peinder, P.C.A. Bruijnincx, B.M. Weckhuysen, J. Catal. 316 (2014) 24–35.

[52] K.D. Bartle, W.R. Ladner, T.G. Martin, C.E. Snape, D.F. Williams, Fuel 58 (1979) 413–422.
[53] T. Suzuki, M. Itoh, Y. Takegami, Y. Watanabe, Fuel 61 (1982) 402–410.
[54] D.A. Netzel, D.R. McKay, R.A. Heppner, F.D. Guffey, S.D. Cooke, D.L. Varie, D.E. Linn, Fuel 60 (1981) 307–320.
[55] M. Ibáñez, M. Artetxe, G. Lopez, G. Elordi, J. Bilbao, M. Olazar, P. Castaño, Appl. Catal. B: Environ. 148-149 (2014) 436–445.
[56] H. Zhang, S. Shao, R. Xiao, D. Shen, J. Zeng, Energy Fuels 28 (2014) 52–57.
[57] I.V. Kozhevnikov, S. Holmes, M.R.H. Siddiqui, Appl. Catal. A Gen. 214 (2001) 47–58.
[58] A.R. Pradhan, J.F. Wu, S.J. Jong, T.C. Tsai, S.B. Liu, Appl. Catal. A Gen. 165 (1997) 489–497.
[59] D.W. Breck, Zeolite Molecular Sieves: Structure, Chemistry and Use, Eds, Wiley, NewYork, 1974, pp. 593–724.
[60] T.M. Davis, C.-Y. Chen, N. Žilková, D. Vitvarová-Procházková, J. Čejka, S.I. Zones, J. Catal. 298 (2013) 84–93.
[61] S. Goel, Z. Wu, S.I. Zones, E. Iglesia, J. Am. Chem. Soc. 134 (2012) 17688–17695.
[62] M. John, K. Alexopoulos, M.-F. Reyniers, G.B. Marin, ACS Catal. 6 (2016) 4081–4094.